COSOLVENT-WATER DISPLACEMENT IN ONE-DIMENSIONAL SOIL COLUMN

By Thomas C. Harmon,[1] Associate Member, ASCE, Tae-Joon Kim,[2] Brian K. Dela Barre,[3] Member, ASCE, and Constantinos V. Chrysikopoulos,[4] Member, ASCE

ABSTRACT: A one-dimensional flow and transport model with dynamic fluid density and viscosity terms is proposed for modeling cosolvent flushing in a water-saturated porous medium. Given knowledge of the density and viscosity functions for cosolvent-water mixtures, the model is controlled by two flow parameters (specific storage and permeability) and one transport parameter (dispersivity). Sensitivity analysis demonstrates that the model solution is relatively insensitive to the flow parameters for the imposed constant head, constant flow conditions. The dynamic density and viscosity model is tested against the conventional transport model in simulating breakthrough data from soil column experiments in which water is displaced by pure methanol pulses (or slugs). Methanol slug breakthrough behavior is first predicted using independent parameter estimates (dispersivity obtained from tracer tests), then the dispersivity was adjusted to obtain optimal fits. The dynamic model provided slightly better predictions than the conventional transport model but failed to accurately reproduce methanol breakthrough behavior. Irregularities in observed slug breakthrough curves suggest that frontal instabilities may have been the cause of the discrepancy between the model and observations. Cosolvent overriding may have also contributed to the discrepancy in the horizontal displacement case.

INTRODUCTION

Miscible, inhomogeneous fluids are mutually soluble fluids with significant density and viscosity differences. A timely example of such a pair involves the flushing of water saturated soils with water-miscible solvents or cosolvents. Cosolvent flushing has been investigated for enhancing subsurface remediation strategies for more than a decade (Rao et al. 1985, 1991; Fu and Luthy 1986a, 1986b; Palmer and Fish 1992; Brandes and Farley 1993; Augustijn et al. 1994; Grubb and Sitar 1994; Luthy et al. 1994; Imhoff et al. 1995). The technology has recently developed to the point of testing at the field scale, where it has yielded promising results (Rao et al. 1997). The approach requires the application of substantial quantities of cosolvents. Thus, understanding the dynamics of cosolvent-water mixing in the subsurface environment is important to avoid wasteful application and/or escape of the cosolvents.

Cosolvent-water displacement problems are similar to those associated with enhanced oil recovery [e.g., Blackwell et al. (1959), Homsy (1987), Lake (1989), and Kempers and Haas (1994)], where the process is more commonly referred to as solvent flooding. Solvent channeling during oil recovery operations can result from permeability stratification, gravity segregation (solvent overriding), and front instability development. While the first two of these processes are relatively straightforward, instability development imposes complex disturbances in the concentration field and requires more detailed description. Instabilities may arise from density and viscosity effects. Density-induced instabilities occur when a more dense fluid overlies a less dense fluid, and the two mix to achieve a stable density gradient. This process is often referred to as Rayleigh convection (Gebhart et al. 1988; Schincariol and Schwartz 1990). Viscosity-induced instabilities occur due to a combination of effects related to the viscosity difference, interstitial velocity, and medium permeability. However, for a given flow regime, instabilities are more likely to occur when a less viscous fluid (e.g., methanol) is displacing a more viscous fluid (e.g., water). An instability in the front begins as a small finger in the displacing fluid that penetrates ahead of the cosolvent-water front due to a local permeability increase. The fingering tends to self-propagate by virtue of its lower resistance to flow. This process is often referred to as viscous fingering (Tan and Homsy 1992; Manickam and Homsy 1993, 1994). The combined effect of the density- and viscosity-driven instabilities is difficult to predict accurately, especially in natural porous media. In a one-dimensional (1D) column study, frontal instability will manifest itself as irregular effluent concentration history.

This work investigates the potential for neglecting cosolvent-water frontal instability phenomena for purposes of computational simplicity. Conventional ground-water flow and contaminant transport model equations are presented with emphasis on dynamic density and viscosity parameters. The resulting model is tested against results from 1D, constant flow soil column experts in which a cosolvent (methanol) pulse displaces water from a homogeneous, sandy medium.

MATHEMATICAL MODEL

The modeling approach employed here assumes that the flow is isothermal and inhomogeneous but that displacement is fully miscible with density and viscosity differences due to concentration fluctuations. The miscible fluid flow equation for vertical 1D flow, in terms of the hydraulic head, is given by (Frind 1982; Huyakorn et al. 1987; Schincariol et al. 1994; Zhang and Schwartz 1995)

$$S_s \frac{\partial h(t, z)}{\partial t} = \frac{\partial}{\partial z}\left\{k_z \frac{\rho_0 g}{\mu(t, z)}\left[\frac{\partial h(t, z)}{\partial z} + \left(\frac{\rho(t, z)}{\rho_0} - 1\right)\right]\right\} \quad (1)$$

where S_s = specific storage; t = time; z = spatial coordinate in the vertical direction; k_z = intrinsic permeability coefficient in the vertical direction; g = gravitational acceleration; ρ_0 = reference density (for clean water); ρ and μ = the density and dynamic viscosity of the water-methanol mixture, respectively; and h = hydraulic head for clean water defined as

[1]Asst. Prof., Dept. of Civ. and Envir. Engrg., Univ. of California, Los Angeles, CA 90095-1593. E-mail: tch@seas.ucla.edu

[2]Grad. Student, Dept. of Civ. and Envir. Engrg., Univ. of California, Irvine, CA 92697-2175.

[3]Grad. Student, Dept. of Civ. and Envir. Engrg., Univ. of California, Los Angeles, CA.

[4]Assoc. Prof., Dept. of Civ. and Envir. Engrg., Univ. of California, Irvine, CA.

Note. Associate Editor: Susan E. Powers. Discussion open until June 1, 1999. To extend the closing date one month, a written request must be filed with the ASCE Manager of Journals. The manuscript for this technical note was submitted for review and possible publication on July 24, 1997. This technical note is part of the ***Journal of Environmental Engineering***, Vol. 125, No. 1, January, 1999. ©ASCE, ISSN 0733-9372/99/0001-0087–0091/$8.00 + $.50 per page. Technical Note No. 16275.

$$h(z, t) = \frac{P(z, t)}{\rho_0 g} + z \tag{2}$$

where P = fluid pressure. The density and viscosity of the mixed fluid are represented by empirical functions of the methanol concentration that are linear and quadratic (i.e., nonmonotonic), respectively. Linear and nonlinear regressions performed on the data of Kikuchi and Oikawa (1967) produced the following relationships:

$$\rho = \rho_0 - 0.25C(t, z) \tag{3}$$

$$\mu = \mu_0 + 2.47C(t, z) - 3.63C^2(t, z) \tag{4}$$

where density, viscosity, and concentration are in terms of grams/cubic centimeter, grams/centimeter minute, and grams/cubic centimeter, respectively. Clean fluid density and viscosity values employed for water and methanol (20°C) were 1.01 and 0.79 g/cm^3 and 0.64 and 0.32 g/(cm·min), respectively.

For vertical 1D methanol transport, the following advection-dispersion equation is applicable:

$$R\frac{\partial C(t, z)}{\partial t} = \frac{\partial}{\partial z}\left[D_z(t, z)\frac{\partial C(t, z)}{\partial z}\right] - \frac{\partial}{\partial z}[U_z(t, z)C(t, z)] \tag{5}$$

where R = retardation factor accounting for methanol adsorption onto the solid matrix under local equilibrium conditions (assumed to be equal to 1 here); and U_z = fluid interstitial velocity in the vertical direction defined by Darcy's law as

$$U_z(t, z) = -\frac{k_z\rho_0 g}{\mu(t, z)\theta}\left[\frac{\partial h(t, z)}{\partial z} + \left(\frac{\rho(t, z)}{\rho_0} - 1\right)\right] \tag{6}$$

where θ = porosity; and D_z = hydrodynamic dispersion coefficient defined as (Bear and Verruijt 1987)

$$D_z(t, z) = \alpha U_z(t, z) + D_e \tag{7}$$

where α = dispersivity of the soil column; $D_e = D/\tau$ = effective molecular diffusion coefficient in the porous media; D = molecular diffusion coefficient; and τ = porous medium tortuosity.

The appropriate initial and boundary conditions for the downward displacement problem are

$$h(0, z) = \frac{P_o}{\rho_0 g} + U_z^{\downarrow}\left(\frac{\mu_0\theta}{k_z\rho_0 g}\right)z \tag{8a}$$

$$h(t, 0) = \frac{P_o}{\rho_0 g} \tag{8b}$$

$$U_z^{\downarrow} = -U_z(t, l) = \frac{k_z\rho_0 g}{\mu(t, l)\theta}\left[\frac{\partial h(t, l)}{\partial z} + \left(\frac{\rho(t, l)}{\rho_0} - 1\right)\right] \tag{8c}$$

where $U_z^{\downarrow} = Q/\theta A$ = constant fluid interstitial velocity in the downward direction; Q = volumetric flow rate regulated by the pump in the experiments; A = cross-sectional area of the column; and l = column length. The condition (8*a*) establishes that initially the hydraulic head increases linearly with elevation from the constant hydraulic head corresponding to the outlet pressure P_o, assuming there is only fresh water in the column. The boundary condition (8*b*) implies that a constant hydraulic head is maintained at the outlet boundary (in this case atmospheric pressure). The boundary condition (8*c*) indicates that the fluid interstitial velocity is constant at the inlet boundary due to the constant volumetric flow rate.

The corresponding initial and boundary conditions for the methanol transport equation (5) are

$$C(0, z) = 0; \quad \frac{\partial C(t, 0)}{\partial z} = 0; \quad C(t, l) = \begin{cases} C_0 & 0 < t < t_p \\ 0 & t > t_p \end{cases} \tag{9a–c}$$

where C_0 = pure methanol concentration; and t_p = pulse duration of methanol injection. The initial condition (9*a*) establishes that there is no initial methanol concentration within the column. The outlet boundary condition (9*b*) preserves concentration continuity at the end of the column. The inlet boundary condition (9*c*) represents a pulse injection of a constant concentration.

For upward flow, the appropriate initial condition corresponding to (8*a*) is obtained by multiplying the second term on the right-hand side by $(l - z)$ instead of z, and by adding l to the entire expression. Boundary condition (8*b*) is rewritten for $h(t, l)$, and l is added to the right-hand side. Boundary (8*c*) is rewritten for $U_z(t, 0)$, and the hydraulic gradient and variable density are evaluated at $z = 0$. The initial condition for upward transport is given by (9*a*). For boundary conditions associated with upward transport, the concentration gradient in (9*b*) is evaluated at l instead of 0, and the pulse injection is set to 0 instead of l.

For horizontal flow, again relative to the equations shown for vertical flow, the buoyancy term $(\rho/\rho_0 - 1)$ drops out of (1), (6), and (8*c*). The appropriate initial condition is obtained from (8*a*) by multiplying the second term on the right-hand side by $(l - z)$ instead of z. The atmospheric pressure boundary condition (8*b*) is rewritten for $h(t, l)$, and influent boundary (8*c*) is rewritten for $z = 0$, the column entrance. The initial and boundary conditions for horizontal transport are the same as those discussed for upward transport.

The solution to the coupled system of equations was obtained numerically by employing the backward finite-difference approximation for the time derivatives (i.e., the fully implicit finite-difference approximation) and the central difference approximation for the spatial derivatives. In numerical simulations, density and concentration terms were averaged between two nodes to moderate large density variations. In addition by using the hydraulic head instead of fluid pressure in numerical simulations, pressure changes were managed in a tolerable range. The miscible fluid flow equation (1) is solved for the hydraulic head distribution, which is required for the determination of the velocity distribution. Subsequently, the velocity distribution is employed in the methanol transport equation (5) to obtain the corresponding methanol concentrations. The procedure is repeated with the estimated methanol concentrations until a stable solution is obtained. The governing partial differential equations (1) and (5) are nonlinear because the density and viscosity are dependent on the methanol concentration, which in turn changes velocity and then the dispersion coefficient. The resulting nonlinear finite-difference equations are sufficiently solved by lagging the nonlinear coefficients (i.e., evaluation of the fluid velocity and dispersion coefficient at the previous time step) so that the finite-difference equations become linear [e.g., Hoffman (1992)].

EXPERIMENTAL METHODS

Conventional miscible displacement tests were conducted using 1D soil columns. First, dilute methanol solutions were used to estimate dispersivity. Then, pure methanol pulses displaced the clean water to produce miscible, inhomogeneous fluid displacement behavior. The former type of test is referred to here as a tracer test, and the latter is referred to as methanol slug test. In enhanced oil recovery parlance [e.g., Brigham et al. (1961)], the slug tests constituted unfavorable displacement conditions at the front of the pulse (displacement of a more viscous fluid by a less viscous fluid), and favorable conditions at the tail of the pulse.

For each experiment a stainless steel column 25.0 cm in length with 2.06-cm inner diameter was employed. The packing material was Borden sand fraction −20+40 (U.S. Std. Mesh). This fraction has a geometric mean diameter of 0.06 cm and a solid density of ~2.7 g/cm^3 (Ball et al. 1990). The

gravimetrically determined porosity of the packed column was 0.35, implying a bulk density of the packing of ~1.75 g/cm^3 and a pore volume of ~30 cm^3. Flow was driven through the soil column using an high-pressure liquid chromatography pump. A syringe pump contained either a dilute methanol solution (tracer tests) or pure methanol (slug tests). In both cases, the labeled methanol (^{14}C-MeOH) was mixed and tested in triplicate for initial activity prior to the experiment. After the prescribed input time, a two-way, electronically actuated switching valve changed the flow from the syringe pump to the high-pressure liquid chromatography pump. The soil column was oriented horizontally for the tracer tests, as density effects were not a concern at the trace levels employed (<0.2 μmole/L). The tracer tests were operated at low (0.02 mL/min), medium (0.24 mL/min) and high (0.92 mL/min) flow rates, which correspond to interstitial velocities of 0.014, 0.17, and 0.66 cm/min, respectively. The slug test was performed at the high velocity only, which was intended to be representative of advection-dominated flow conditions expected for a hydraulically controlled cosolvent flushing operation.

Effluent samples were dispensed via an autosampler into sample vials just below the surface of the liquid scintillation fluid. Each sample was capped and shaken immediately after collection to minimize volatilization losses. Samples at low, medium, and high flow rates were collected every 60, 5.3, and 1.3 min, respectively. The volume collected was determined gravimetrically for the tracer tests. All samples were quantified by liquid scintillation counting. Measured methanol concentrations for the tracer and slug tests were assembled in the form of breakthrough curves and integrated to evaluate mass conservation. The most probable causes of loss were volatilization at the collection and truncation of the effluent methanol due to point sampling as opposed to a continuous monitoring. The mass recovery ranged from 91 to 98% of the input mass.

RESULTS AND ANALYSIS

Prior to modeling the methanol slug breakthrough curves, the parameters for flow (permeability and specific storage) and transport (dispersivity) were independently estimated using a combination of experimental techniques and model sensitivity analysis. The results from the tracer tests were used to determine the dispersivity characterizing soil column under miscible, homogeneous displacement conditions. The observed breakthrough response was analyzed using the analytical solution to the 1D advection-dispersion equation (van Genuchten and Alves 1982). For the three tracer-test flow rates employed, nonlinear regression procedures provided a dispersivity estimate of 0.14 cm (±0.02 cm) for the tracer results. The fits (not shown here) were good for all three velocities, and there was no observable retardation of the methanol pulses. The soil column permeability estimated using a constant head permeameter was 1.2×10^{-8} cm^2 ($\pm 2 \times 10^{-9}$ cm^2). Adjusting the specific storage value to 2.7×10^{-6} cm^{-1} ($\pm 2.0 \times 10^{-7}$ cm) optimized the present model's agreement with the data from the three tracer tests.

The two flow parameters, permeability and specific storage, were expected to exert a relatively weak influence on methanol slug behavior because of the imposed constant flow conditions. A parameter sensitivity analysis was carried out in which the basis for comparison was the simulation for dispersivity, permeability and specific storage values of 0.10 cm, 1.0×10^{-8} cm^2, and 1.0×10^{-6} cm^{-1}, respectively. Breakthrough curve simulations for the downward flow orientation are shown in Fig. 1 and were generated by varying the specific storage [Fig. 1(a)], permeability [Fig. 1(b)], and dispersivity [Fig. 1(c)]. In each case, the two remaining parameters were held constant at the aforementioned values while the target parameter was adjusted. Results from the sensitivity analysis confirmed that,

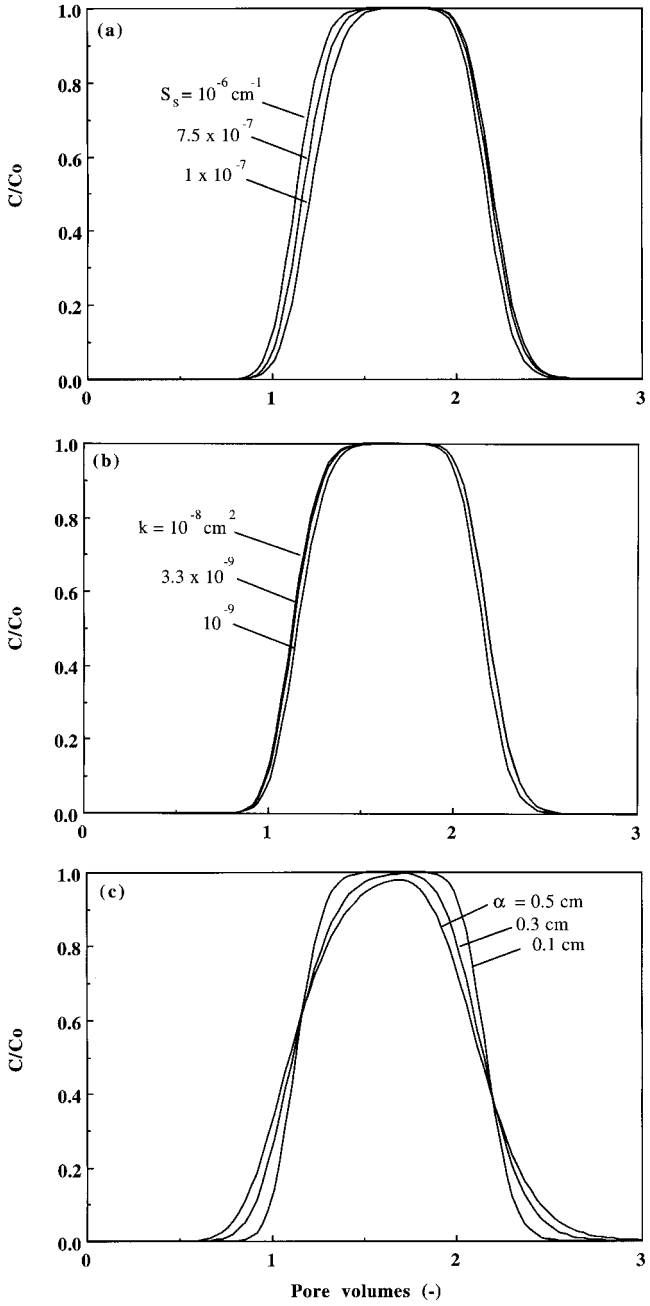

FIG. 1. Model Sensitivity Analysis Simulations Depicting Methanol Slug Breakthrough Responses for: (a) Specific Storage; (b) Permeability; (c) Dispersivity Values

for the parameter ranges of interest, the coupled flow and transport model solution is most sensitive to changes in the dispersivity value and relatively insensitive to changes in permeability and specific storage values.

The observed breakthrough curves for the three displacement configurations are shown in Fig. 2, along with predicted and fitted model simulations. As noted in the figure caption, both the dynamic density and viscosity and the conventional convective dispersion models were used to predict slug test behavior using the tracer-based dispersivity value. In terms of the sum of the squared error (SSE) for the simulations versus data, the accuracy of both model predictions was about the same for the downward displacement case. For upward displacement, the variable density and viscosity model prediction (SSE = 0.78) was substantially better than that of the conventional model (SSE = 1.15). For horizontal displacement, the variable density and viscosity model prediction (SSE = 1.43)

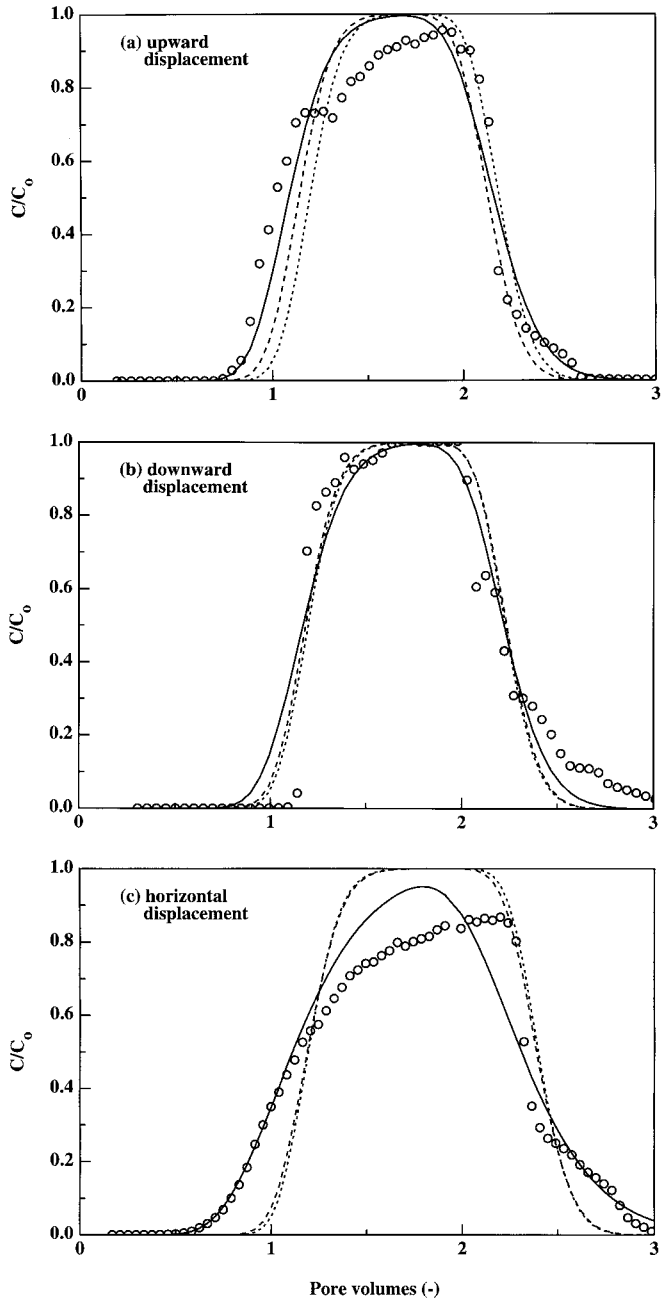

FIG. 2. Observed (○) and Simulated Methanol Slug Breakthrough Responses for: (a) Upward Flow Conditions; (b) Downward Flow Conditions; (c) Horizontal Flow Conditions. – – – Represents Predictive Dynamic Density and Viscosity Model Simulations with Tracer-Base Dispersivity Value [α = 0.14 cm; SSE = (a) 0.78, (b) 0.53, (c) 1.43]; . . . . . Represents Predictive Conventional Convective Dispersion Model Simulations with Tracer-Based Dispersivity Value [α = 0.14 cm; SSE = (a) 1.15, (b) 0.54, (c) 1.58; —— Represents Simulations in Which Dispersivity Was Fitted [α = (a) 0.30, (b) 0.29, (c) 0.95 cm; SSE = (a) 0.41, (b) 0.53, (c) 0.52]

was slightly better than that of the conventional model (SSE = 1.58).

Under stable displacement conditions, regular (i.e., smooth) breakthrough behavior is expected, and it is common to account for deviation from tracer behavior by adjusting the dispersivity (Brigham et al. 1961; Buès and Aachib 1991; Kempers and Haas 1994). The degree of departure from tracer-type dispersion depends on the viscosity and density differences as well as the velocity at which displacement occurs and the medium permeability (Brigham et al. 1961). These effects can be summarized in terms of the mobility ratio (M = viscosity of displaced fluid/viscosity of displacing fluid) and the gravity number

$$N_g = \frac{k_z g(\rho_p - \rho_i)\sin \phi}{\mu_p \theta U_z} \tag{10}$$

Here, the M values are approximately 2.0 and 0.5 for the front and tail of the slug, respectively. The N_g values for the front and tail are roughly 0.06 and 0.12, respectively. In a water/brine displacement test performed under similar conditions (M = 0.83 and N_g = 0.066), with flow controlled to maintain stable conditions, Kempers and Haas (1994) observed conventional convection dispersion behavior. Here, the upward tail and downward front displacement results in Figs. 2(a and b) suggest behavior that is described reasonably well by the tracer-based dispersivity. However, the simulations were unable to predict the irregular behavior of the upward front, upward peak, and downward tail. Optimally fitted dispersivity values created slight improvements for the vertical cases but also failed to capture these irregularities. Such irregularities are characteristic of frontal instabilities.

The observed horizontal slug test's breakthrough behavior deviates most significantly from tracer-like behavior [Fig. 2(c)]. The dynamic density and viscosity model's adjusted fit results in a marked improvement over the predictions and succeeds in capturing the dynamics of the front and tail of the observed breakthrough curve. However, this optimized fit clearly fails to reproduce the pulse peak.

There are several plausible explanations for the proposed model's failure to adequately describe the observed behavior. First, unstable displacement behavior seemed to develop as a result of the constant and elevated flow rate. Second, for the horizontal results, it is also probable that the irregular breakthrough behavior was caused by density-induced overriding of the methanol pulse through the upper portion of the column. The present model could be adapted to describe overriding but would require a two- or three-dimensional formulation with variable head boundary conditions. Frontal instabilities may also have contributed to the present model's inadequate performance for the horizontal test case.

CONCLUDING REMARKS

This work tests a modeling approach for addressing the problem of cosolvent injection in water-saturated porous media. Engineers focusing on the residual contaminant aspect of the flushing problem may be inclined to model contaminant behavior using conventional 1D miscible, homogeneous fluid displacement model. For the experimental results presented here, the proposed miscible, inhomogeneous displacement model did improve slightly upon the conventional approach. Unfortunately, the constant head and flow conditions imposed in the experiments precluded extensive testing of the proposed model. Because the inhomogeneous displacement model is a more general form of the conventional model typically applied to ground-water flow and contaminant transport problems, a prominent recommendation that follows is a precaution against the conventional approach. Well-to-well injection-extraction conditions in confined zones may induce frontal instabilities, particularly at reasonably high pore-water velocities and/or in the face of natural permeability variations. The results here support the notion that simulation of the cosolvent flushing problem in a confined geological unit may require more complex models capable of supporting dynamic density and viscosity conditions in two- or three-dimensions. Models capable of addressing the problem of frontal instabilities may also be necessary, depending on the scale of the flushing zone and the desired accuracy of the modeling effort.

ACKNOWLEDGMENTS

This work was sponsored by the University of California Energy Institute (Award No. UER-299), by the U.S. Environmental Protection Agency Office of Exploratory Research (Grant No. R-823579-01-0) and by the University of California, Irvine, through an allocation of computer resources on the UCI SPP2000. The content of this manuscript does not necessarily reflect the views of these organizations and no official endorsement should be inferred.

APPENDIX I. REFERENCES

Augustijn, D. C. M., Jessup, R. E., Rao, P. S. C., and Wood, A. L. (1994). ''Remediation of contaminated soils by solvent flushing.'' *J. Envir. Engrg.*, ASCE, 120(1), 42–57.

Ball, W. P., Buehler, C., Harmon, T. C., and Mackay, D. M. (1990). ''Characterization of a sandy aquifer material at the grain scale.'' *J. Contam. Hydrol*., 5(3), 253–259.

Bear, J., and Verruijt, A. (1987). *Modeling groundwater flow and pollution.* Reidel, Dordrecht, The Netherlands.

Blackwell, R. J., Rayne, J. R., and Terry, W. M. (1959). ''Factors influencing the efficiency of miscible displacement.'' *Petrol. Trans.*, AIME, 217, 1–8.

Brandes, D., and Farley, K. J. (1993). ''Importance of phase behavior on the removal of residual DNAPLs from porous media by alcohol flooding.'' *Water Envir. Res.*, 65(7), 869–878.

Brigham, W. E., Reed, P. W., and Dew, J. N. (1961). ''Experiments on mixing during miscible displacement in porous media.'' *Soc. Petroleum Engrg. J.*, 3, 1–8.

Buès, M. A., and Aachib, M. (1991). ''Influence of the heterogeneity of the solutions on the parameters of miscible displacement in saturated porous medium. Part 1: Stable displacement with density and viscosity contrasts.'' *Experiments Fluid Mech.*, 11, 25–32.

Frind, E. O. (1982). ''Simulation of long-term transient density-dependent transport in groundwater.'' *Adv. Water Resour.*, 5, 73–88.

Fu, J. K., and Luthy, R. G. (1986a). ''Aromatic compound solubility in solvent/water mixtures.'' *J. Envir. Engrg.*, ASCE, 112, 328–345.

Fu, J. K., and Luthy, R. G. (1986b). ''Effect of organic solvent on sorption of aromatic solutes onto soils.'' *J. Envir. Engrg.*, ASCE, 112, 346–366.

Gebhart, B., Jaluria, Y., Mahajan, R. L., and Sammakia, B. (1988). *Buoyancy-induced flows and transport*. Hemisphere/Harper and Row, New York.

Grubb, D. G., and Sitar, N. (1994). ''Evaluation of technologies for in situ cleanup of DNAPL contaminated sites.'' *Rep. No. EPA/600/R-94/120*, U.S. Environmental Protection Agency, Washington, D.C.

Hoffman, J. D. (1992). *Numerical methods for engineers and scientists.* McGraw-Hill, New York, 825.

Homsy, G. M. (1987). ''Viscous fingering in porous media.'' *Ann. Rev. Fluid Mech.*, 19, 271–301.

Huyakorn, P. S., Andersen, P. F., Mercer, J. W., and White, H. O., Jr. (1987). ''Saltwater intrusion in aquifers: Development and testing of a three-dimensional finite element model.'' *Water Resour. Res.*, 23(2), 293–312.

Imhoff, P. T., Gleyzer, S. N., Mcbride, J. F., Vancho, L. A., Okuda, I., and Miller, C. T. (1995). ''Cosolvent-enhanced remediation of residual dense nonaqueous phase liquids: Experimental investigation.'' *Environ. Sci. and Technol.*, 29(8), 1966–1976.

Kempers, L. J. T. M., and Haas, H. (1994). ''The dispersion zone between fluids with different density and viscosity in a heterogeneous porous medium.'' *J. Fluid Mech.*, Cambridge, England, 267, 299–324.

Kikuchi, M., and Oikawa, E. (1967). ''Viscosities of alcohol-water mixtures.'' *Nippon Kagaku Zasshi*, Tokyo, 88, 1259–1267.

Lake, L. W. (1989). *Enhanced oil recovery.* Prentice-Hall, Englewood Cliffs, N.J.

Luthy, R. G., et al. (1994). ''Remediating tar-contaminated soils at manufactured gas plant sites.'' *Environ. Sci. and Technol.*, 28(6), A266–A276.

Manickan, O., and Homsy, G. M. (1993). ''Stability of miscible displacements in porous media with nonmonotonic viscosity profiles.'' *Phys. Fluids A*, 5(6), 1356–1357.

Manickam, O., and Homsy, G. M. (1994). ''Simulation of viscous fingering in miscible displacements with nonmonotonic viscosity profiles.'' *Phys. Fluids*, 6(1), 95–107.

Palmer, C. D., and Fish, W. (1992). ''Chemical enhancements to pump-and-treat remediation.'' *Rep. No. EPA/540/S-92/001*, U.S. Environmental Protection Agency, Washington, D.C.

Rao, P. S. C., Hornsby, A. G., Kilcrease, D. P., and Nkedi-Kizza, P. (1985). ''Sorption and transport of hydrophobic organic chemicals in aqueous and mixed solvents systems: Model development and preliminary evaluation.'' *J. Envir. Quality*, 14, 376–383.

Rao, P. S. C., Lee, L. S., and Wood, A. L. (1991). ''Solubility, sorption and transport of hydrophobic organic chemicals in complex mixtures.'' *Rep. No. EPA/600/M-91/009*, U.S. Environmental Protection Agency, Washington, D.C.

Rao, P. S. C., et al. (1997). ''Field-scale evaluation of in situ cosolvent flushing for enhanced aquifer remediation.'' *Water Resour. Res.*, (33)12, 2673–2686.

Schincariol, R. A., and Schwartz, F. W. (1990). ''An experimental investigation of variable density flow and mixing in homogeneous and heterogeneous media.'' *Water Resour. Res.*, 26(10), 2317–2329.

Schincariol, R. A., Schwartz, F. W., and Mendoza, C. A. (1994). ''On the generation of instabilities in variable density flow.'' *Water Resour. Res.*, 30(4), 913–927.

Tan, C. T., and Homsy, G. M. (1992). ''Viscous fingering with permeability heterogeneity.'' *Phys. Fluids A*, 4(6), 1099–1101.

van Genuchten, M. Th., and Alves, W. J. (1982). ''Analytical solutions of the one-dimensional convective-dispersive solute transport equation.'' *Tech. Bull. No. 1661*, U.S. Department of Agriculture, Riverside, Calif.

Zhang, H., and Schwartz, F. W. (1995). ''Multispecies contaminant plumes in variable density flow systems.'' *Water Resour. Res.*, 31(4), 837–847.

APPENDIX II. NOTATION

The following symbols are used in this paper:

A = cross-sectional area of column (L^2);
C = methanol concentration in mixed fluid (ML^{-3});
C_0 = pure methanol concentration (ML^{-3});
D = molecular diffusion coefficient ($L^2\ t^{-1}$);
D_e = effective molecular diffusion coefficient, equal to D/τ ($L^2\ T^{-1}$);
D_z = hydrodynamic dispersion coefficient in z direction ($L^2\ T^{-1}$);
d = column diameter (L);
g = gravitational acceleration ($L\ T^{-2}$);
h = hydraulic head for fresh ground water (L);
k_z = intrinsic permeability in z direction (L^2);
l = column length (L);
P = fluid pressure ($ML^{-1}\ T^{-2}$);
P_o = pressure at outlet boundary ($ML^{-1}\ T^{-2}$);
Q = volumetric flow rate ($L^3\ T^{-1}$);
R = retardation factor;
S_s = specific storage (L^{-1});
t = time (T);
t_p = duration of methanol pulse (T);
U_z = fluid interstitial velocity in z direction, defined in Eq. (6) ($L\ T^{-1}$);
$U_z^{\downarrow}$ = constant fluid interstitial velocity in downward direction ($L\ T^{-1}$);
z = spatial coordinate in longitudinal direction of column (L);
α = dispersivity (L);
θ = porosity (i.e., liquid volume/porous medium volume) ($L^3\ L^{-3}$);
μ = dynamic viscosity of mixed fluid, defined in Eq. (4) ($ML^{-1}\ T^{-1}$);
μ_m = dynamic viscosity of pure methanol ($ML^{-1}\ T^{-1}$);
μ_p = dynamic viscosity of production or displaced fluid ($ML^{-1}\ T^{-1}$);
μ_0 = dynamic viscosity of fresh water ($ML^{-1}\ T^{-1}$);
ρ = density of mixed fluid, defined in Eq. (3) (ML^{-3});
ρ_i = density of injected or displacing fluid (ML^{-3});
ρ_p = density of production or displaced fluid (ML^{-3});
ρ_0 = density of fresh water (ML^{-3});
τ = tortuosity; and
ϕ = angle between displacement direction and horizontal.